Using Real-Time Kinematics Algorithm in Mission Critical Communication for Accurate Positioning and Time Correction over 5G and Beyond Networks

Mutasem Q. Hamdan*, Chuan Heng Foh*, Atta ul Quddus*, Stephen Hancock†, Oliver Holland‡, Richard Woodling†
*5GIC & 6GIC, Institute for Communication Systems (ICS), University of Surrey, Guildford, United Kingdom
{Mutasem.hamdan, c.foh, a.quddus}@surrey.ac.uk
†Ordnance Survey, United Kingdom
{stephen.hancock, richard.woodling}@os.uk
‡AWTG LTD, United Kingdom
oliver.holland@awtg.co.uk

***Abstract*—At 5G and beyond networks, accurate localization services and nanosecond time synchronization are crucial to enabling mission-critical wireless communications technologies and techniques such as autonomous vehicles and distributed multiple-input and multiple-output (MIMO) antenna systems. This paper investigates how to improve wireless time synchronization by studying time correction based on the Real-Time Kinematics (RTK) positioning algorithm. Using the multiple Global Navigation Satellite System (GNSS) receiver references and the proposed binary GNSS satellite formation to reduce the effect of the ionosphere and troposphere delays and recede the measurement phase-range and pseudorange errors. As a result, it improves user equipment's (UE) localization and measures the time difference between the Base Station (BS) and the UE local clocks. The results show that the positioning accuracy has been increased, and a millimetre accuracy has been achieved while attaining the sub-nanosecond time error (TE) between the UE's and BS local clocks.**

***Index Terms*—RTK, Time synchronization, Time error, Binary satellites, 5G, Baseband Unit (BBU), Ambiguity number.**

I. Introduction

High-precision global positioning system (GPS) real-time kinematics (RTK) positioning is extensively used in land, sea, and air surveying and navigation applications. However, in time synchronization applications such as 4G and 5G networks such as critical Internet of Things (IoT), where data latency is less than 50ms and reliability is higher than 99.9%, mainly the Global Navigation Satellite System (GNSS) and Precision Time Protocol (PTP) are mainly under research at the Base Station (BS) side only [1][2][3]. The RTK technique uniqueness depends on sending a correction observation message to the user equipment's (UE) GNSS receiver through wireless technology from an accurate reference such as the GNSS receiver at the BS, which improves the UE's positioning accuracy and measures the Time Error (TE) between the UE and BS clocks to improve the synchronization for critical missions and real-time application in 6G. For example, in autonomous cars, for critical missions, group coordination is the backbone for mission success and avoiding collisions or diversion from the targets, which requires highly accurate synchronization between all the On-Board Units (OBU) in the vehicles group. . The distance from the UE receiver to the BS reference receiver may range from a few kilometers to hundreds of kilometers. Even positioning with a short baseline distance between the UE and the BS receivers provides a theoretical positioning for UE in millimeter accuracy and a sub-nanosecond time error between the clocks. In practice, it shows that the achievable is within decimeters and centimeters under field conditions and with synchronization of several nanoseconds out of time [4][5]. The problem of accounting for distance-dependent biases between the system elements, which are: the satellite transmitters, UE and BS receivers, grows and, as a consequence, reliable ambiguity resolution for the number of cycles between each satellite and both UE and BS receivers for the same frequency band becomes an even more significant challenge. However, the Double Difference (DD) technique can help avoid residual biases or errors when the distance between the two GNSS receivers is less than 1 km [5]. For baselines greater than 10 Km, increasing the distance causes significant ionospheric tropospheric delays, and the orbital error becomes significant [6]. Additionally, when GPS signals are continuously tracked and no loss of lock occurs, the integer ambiguities resolved at the beginning of a survey can be kept for the entire user kinematic positioning span. However, GPS satellite signals may occasionally be shaded by buildings, jammed by other signals, or even blocked inside a building or tunnel. Generally speaking, the integer ambiguity values are not available and must be re-calculated in such cases. These calculations can take from a few tens of seconds to several minutes [7]. As a result, time correction and synchronization accuracy will be affected. In distributed wireless networks, the level of time synchronization should

This work was supported by Innovate UK [Project No: 10011721]. We would also like to acknowledge the support of the University of Surrey 5GIC & 6GIC (https://www.surrey.ac.uk/institute-communication-systems/5g-6g-innovation-centre) members for this work.

be within several nanoseconds [8]. Some effort has been recently showing the potential of using the carrier phase-based synchronization [9]. However, to provide a new method based on the RTK that helps in increasing the short baseline accuracy to better than a millimeter, we propose an algorithm that takes into consideration the spatial distribution of the references and satellites in the perspective of the user so that the errors due to the baseline distances, delays of ionosphere and troposphere can be corrected using statistical approach.

Our main contributions are summarized as follows:

- Propose to use the existing infrastructure of the 4/5G base station GNSS receiver as a reference and use the mobile network to provide UE with observation messages to improve the positioning accuracy of UE and the time synchronization between the local clocks of the BS and UE.
- Propose new selection criteria for optimal satellite formation to reduce the effect of phase range measurement errors. In this proposal, the selection of a binary satellite system depends not only on signal strength and elevation but also on azimuth with respect to the UE and BS GNSS antennas.
- Propose to use more than one reference with symmetrical distribution around the UE GNSS antenna to provide more than one solution. The final solution for the position and TE takes the expectation of all individual solutions to reduce ambiguity calculation errors.

II. System Model

In this article, the system model has M Base References R located in 4/5G BS and serving the UE User Rover U and each R, the observation message is available at R through the 4/5G wireless network connection as in **Fig.4**.

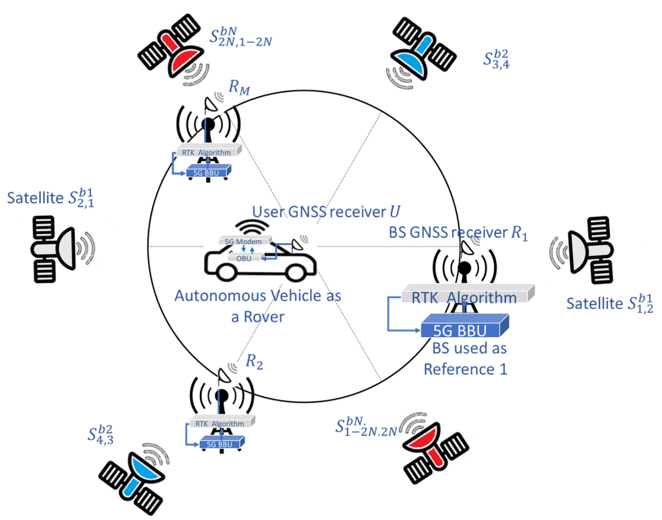

Fig. 1. System Model for Multi-Reference RTK Algorithm

The positioning and TE are based on the following assumptions, many Rs around the U are available, and a subset of only M will be used in the calculation procedure. The U is in the center, and the Rs are equally far from each other. The second assumption is that there are many satellites in the view of the UR, and a special formation will be used that depends on the signal strength elevation and the binary condition. The definition of binary conditions is a system consisting of two satellites that orbit Earth, while U view each of the satellites at opposite azimuths, for instants, in **Fig.4** $S^{1,2}_{b_1}$ is the binary satellite with $S^{1,2}_{b_1}$ and the azimuth from the U perspective is 0 and π, respectively. In the case of the pseudo-range calculation, two binary satellite systems are required. However, in practice, the system may not satisfy such conditions, the best two semi-binary satellite systems can be used. The following equations will describe the model and explain the reasons behind the assumptions. To calculate the pseudo-range $P^{S^{b_n}_{2n-1,2n}}_{R_m,L_i}$ between satellite $S^{b_n}_{2n-1,2n}$ and the R_m for frequency band L_i

$$P^{S^{b_n}_{2n-1,2n}}_{R_m,L_i} = c(t_{R_m} - t^{S^{b_n}_{2n-1,2n}}) \tag{1}$$

Similarly, the pseudorange $P^{S^{b_n}_{2n-1,2n}}_{U,L_i}$ between satellite $S^{b_n}_{2n-1,2n}$ and U for the frequency band L_i:

$$P^{S^{b_n}_{2n-1,2n}}_{U,L_i} = c(t_U - t^{S^{b_n}_{2n-1,2n}}) \tag{2}$$

where t_{R_m}, t_U and $t^{S^{b_n}_{2n-1,2n}}$ are the signal reception time measured by the R_m, U clocks and the measured signal transmission time measured by the satellite clock $S^{b_n}_{2n-1,2n}$ in seconds, respectively. The n is the binary formation number of two satellites and the c is the speed of light. The previous equation can be also written using geometrical range $\rho^{S^{b_n}_{2n-1,2n}}_{R_m,L_i}$ [10]:

$$\begin{aligned} P^{S^{b_n}_{2n-1,2n}}_{R_m,L_i} = \rho^{S^{b_n}_{2n-1,2n}}_{R_m} + c(\delta t_{R_m} - \delta t^{S^{b_n}_{2n-1,2n}}) + I^{S^{b_n}_{2n-1,2n}}_{R_m,L_i} \\ + T^{S^{b_n}_{2n-1,2n}}_{R_m} + \varepsilon_P \end{aligned} \tag{3}$$

where δt_{R_m} and $\delta t^{S^{b_n}_{2n-1,2n}}$ are the U and $S^{b_n}_{2n-1,2n}$ clock biases, respectively. The $I^{S^{b_n}_{2n-1,2n}}_{R_m,L_i}$ and $T^{S^{b_n}_{2n-1,2n}}_{R_m}$ are the ionosphere and troposphere delay effect, respectively . While the ε_P is the measurement error of the pseudo range.

Similarly, the geometric range $\rho^{S^{b_n}_{2n-1,2n}}_{U}$:

$$\begin{aligned} P^{S^{b_n}_{2n-1,2n}}_{U,L_i} = \rho^{S^{b_n}_{2n-1,2n}}_{U} + c(\delta t_U - \delta t^{S^{b_n}_{2n-1,2n}}) + I^{S^{b_n}_{2n-1,2n}}_{U,L_i} \\ + T^{S^{b_n}_{2n-1,2n}}_{U} + \varepsilon_P \end{aligned} \tag{4}$$

In addition, the carrier phase measurement model that shows the phase difference between R_m and $S^{b_n}_{2n-1,2n}$ is :

$$\phi^{S^{b_n}_{2n-1,2n}}_{R_m,L_i} = \phi_{R_m,L_i} - \phi_{S^{b_n}_{2n-1,2n}} + N^{S^{b_n}_{2n-1,2n}}_{R_m,L_i} + \varepsilon_\phi \tag{5}$$

where ϕ_{R_m,L_i} is the measured phase of R_m receiver local oscillator of L_i at time t_{R_m} and $\phi_{S^{b_n}_{2n-1,2n}}$ is the satellite phase measured at time $t^{S^{b_n}_{2n-1,2n}}$, ε_ϕ is the carrier phase measurement error and $N^{S^{b_n}_{2n-1,2n}}_{R_m,L_i}$ is the carrier phase integer ambiguity according to [10] :

$$\phi^{S^{b_n}_{2n-1,2n}}_{R_m,L_i} = \frac{c}{\lambda_{L_i}}(t_{R_m} - t^{S^{b_n}_{2n-1,2n}}) + \frac{c}{\lambda_{L_i}}(\delta t_{R_m} - \delta t^{S^{b_n}_{2n-1,2n}}) + \phi^{(0)}_{R_m,L_i} - \phi^{(0)}_{S^{b_n}_{2n-1,2n}} + N^{S^{b_n}_{2n-1,2n}}_{R_m,L_i} + \varepsilon_\phi \tag{6}$$

where $\phi^{(0)}_{R_m,L_i}$ and $\phi^{(0)}_{S^{b_n}_{2n-1,2n}}$ are the initial phases of the L_i band signal of the satellite transmitter $S^{b_n}_{2n-1,2n}$ and base reference R_{m,L_i} local oscillators and the initial time t_o signal. similarly for the user U GNSS receiver :

$$\phi^{S^{b_n}_{2n-1,2n}}_{U,L_i} = \frac{c}{\lambda_{L_i}}(t_U - t^{S^{b_n}_{2n-1,2n}}) + \frac{c}{\lambda_{L_i}}(\delta t_U - \delta t^{S^{b_n}_{2n-1,2n}}) + (\phi^{(0)}_{U_{L_i}} - \phi^{(0)}_{S^{b_n}_{2n-1,2n}} + N^{S^{b_n}_{2n-1,2n}}_{U,L_i}) + \varepsilon_\phi \tag{7}$$

and the term $B^{S^{b_n}_{2n-1,2n}}_{R_m,L_i} = \phi^{(0)}_{U_{L_i}} - \phi^{(0)}_{S^{b_n}_{2n-1,2n}} + N^{S^{b_n}_{2n-1,2n}}_{U,L_i}$ is the carrier phase bias. This leads to the measurement of the phase range $\Phi_{R_{m,L_i}}$ for L_i is the carrier phase multiplied by the carrier wavelength λ_{L_i} [10]:

$$\Phi^{S^{b_n}_{2n-1,2n}}_{R_{m,L_i}} = \lambda_{L_i}\phi^{S^{b_n}_{2n-1,2n}}_{R_{m,L_i}} \tag{8}$$

From **Eq. 3** and **Eq. 8** of the pseudorange, carrier phase range, and with the use of carrier phase bias $B^{S^{b_n}_{2n-1,2n}}_{R_{m,L_i}}$ and carrier correction $\delta\Phi^{S^{b_n}_{2n-1,2n}}_{R_{m,L_i}}$ terms to take into account the antenna phase center, earth tides, and the wind-up of the phase to formulate the relation between the geometrical range $\rho^{S^{b_n}_{2n-1,2n}}_{R_m}$ and carrier-phase range $\Phi^{S^{b_n}_{2n-1,2n}}_{R_{m,L_i}}$ as:

$$\Phi^{S^{b_n}_{2n-1,2n}}_{R_{m,L_i}} = \rho^{S^{b_n}_{2n-1,2n}}_{R_m} + c(\delta t_{R_m} - \delta t^{S^{b_n}_{2n-1,2n}}) - I^{S^{b_n}_{2n-1,2n}}_{R_m,L_i} + T^{S^{b_n}_{2n-1,2n}}_{R_m} + \lambda_{L_i}B^{S^{b_n}_{2n-1,2n}}_{R_{m,L_i}} + \delta\Phi^{S^{b_n}_{2n-1,2n}}_{R_{m,L_i}} + \varepsilon_\Phi \tag{9}$$

where [10]:

$$\delta\Phi^s_{r,L_i} = -\boldsymbol{d}^T_{r,pco,L_i}\boldsymbol{e}^s_{r,enu} + (\boldsymbol{E}^s\boldsymbol{d}^s_{pco,L_i})^T\boldsymbol{e}^s_r + d_{r,pcv,L_i}(El) + d^s_{pcv,L_i}(\theta) - \boldsymbol{d}^T_{r,disp}\boldsymbol{e}^s_{r,enu} + \lambda_{L_i}\phi_{pw} \tag{10}$$

with the definitions:

- $\boldsymbol{d}_{r,pco,L_i}$: receiver antenna phase center offset in local coordinates.
- $\boldsymbol{e}^s_{r,enu}$: LOS vector from receiver antenna to satellite in local coordinates
- $\boldsymbol{E}^s$: coordinates rotation matrix from ECEF to satellite body-fixed coordinates.
- $\boldsymbol{d}^s_{pco,L_i}$: satellite antenna phase center offset in satellite body-fixed coordinates.
- $\boldsymbol{e}^s_r$: LOS vector from receiver antenna to satellite in ECEF
- $d_{r,pcv,L_i}(El)$: receiver antenna phase center variation
- $d^s_{pcv,L_i}(\theta)$: satellite antenna phase center variation
- $\boldsymbol{d}_{r,disp}$: displacement by the tides of the earth at the receiver position at local coordinates
- ϕ_{pw}: wind-up effect of the phase

Similarity for U:

$$\Phi^{S^{b_n}_{2n-1,2n}}_{U_{L_i}} = \rho^{S^{b_n}_{2n-1,2n}}_{U} + c(\delta t_U - \delta t^{S^{b_n}_{2n-1,2n}}) + I^{S^{b_n}_{2n-1,2n}}_{U,L_i} + T^{S^{b_n}_{2n-1,2n}}_{U} + \lambda_{L_i}B^{S^{b_n}_{2n-1,2n}}_{U_{L_i}} + \delta\Phi^{S^{b_n}_{2n-1,2n}}_{U_{L_i}} + \varepsilon_\Phi \tag{11}$$

III. RTK solution using the Double Difference (DD) and Single Difference (SD) method

The Double Difference (DD) measurement model for baseline less than one km between U and the R_m for signal band L_i using the binary satellites $S^{b_n}_{2n-1,2n}$ and $S^{b_n}_{2n,2n-1}$can be described by the two following equations:

$$\begin{aligned} \Phi^{S^{b_n}}_{UR_m,L_i} &= (\Phi^{S^{b_n}_{2n-1}}_{U_{L_i}} - \Phi^{S^{b_n}_{2n-1}}_{R_{m,L_i}}) - (\Phi^{S^{b_n}_{2n}}_{U_{L_i}} - \Phi^{S^{b_n}_{2n}}_{R_{m,L_i}}) \\ &= \rho^{S^{b_n}}_{UR_m} + \lambda_{L_i}(B^{S^{b_n}_{2n-1}}_{UR_{mL_i}} - B^{S^{b_n}_{2n}}_{UR_{mL_i}}) \\ &\quad + \delta\Phi^{S^{b_n}_{2n-1,2n}}_{U_{L_i}} + \varepsilon_\Phi \end{aligned} \tag{12}$$

Similarly, for the pseudo-range:

$$P^{S^{b_n}}_{UR_m,L_i} = \rho^{S^{b_n}}_{UR_m} + \varepsilon_P \tag{13}$$

It is important to emphasise that each R_m has a well-known stationary and accurate ECEF location r_{R_m}, while the r_U it does not. So the classical RTK targets improving the r_U accuracy using the observations and corrections the R_m sends through the 5G network to the U. Once the measurement vector from **Eq. 12** and **Eq. 13**: $\mathbf{y} = (\boldsymbol{\Phi_{L_1},...,\Phi_{L_i},...,\Phi_{L_I},P_{L_1},...,P_{L_i},...,P_{L_I}})$ observed per binary satellite system per reference U. The classical extended Kalman filter (EKF) uses **y(x)** to calculate the matrix of the partial derivatives $\boldsymbol{Y(x)=\frac{\partial y(x)}{\partial x}}$ and write the measurement error covariance matrix **R** to solve the unknown state vector **x** of the unknown model parameters and the covariance matrix **Cov**. Where $\mathbf{x} = (r_U, v_U, B_{U,R_m,L_1}, ..., B_{U,R_m,L_I})$ contains the position of the user receiver antenna U at the epoch time t_k in ECEF r_U, the velocity of the receiver antenna v_U at the epoch time t_k and $\boldsymbol{B_i} = (B^1_{UR_{m,L_i}}, ..., B^m_{UR_{m,L_i}})$ is the SD carrier phase bias SD. With the user U kinematic mode such as the autonomous cars the time update for the EKF is taking in consideration $\boldsymbol{e}^s_r$,,the standard deviation of L_i the phase-range σ^s_{Φ,L_i} and the pseudo-range σ^s_{P,L_i}. In addition to the updating of EKF time, the U velocity system east, north, and up noises (σ_{ve},σ_{vn},σ_{vu}) between the epochs t_k and t_{k+1} are considered as well. Once the estimated states are calculated, the EKF applies the float carrier phase ambiguity as a new variable in the unknown states $\mathbf{x} = (\boldsymbol{r_U,v_U,N_{U,R_m}})$ to predict $\boldsymbol{\hat{N}_{U,R_m}}$, which will be next used in the modified Lambda algorithm to solve the integer ambiguity of the integer least square (ILS) problem and find $\boldsymbol{\dot{N}_{U,R_m}}$. The produced $\dot{N}_{U,R_m}$ use $(\boldsymbol{\hat{r},\hat{v}})^T Q_{NR} Q_N^{-1}(\dot{(N)} - \hat{N})$ to calculate the accurate $\dot{\boldsymbol{r}}_U$ and $\dot{\boldsymbol{v}}_U$ [10]. In this paper, the EKF, the EKF time update and the resolution of integer ambiguity using modified lambda algorithms [11][12] are beyond the scope and have been used according to [10]. Lastly, the corrected position and the resolution of the integer ambiguity are updated $(\hat{r}_U, \hat{v}_U, \hat{N}_{U,R_m})^T \rightarrow (\dot{r}_U, \dot{v}_U, \dot{N}_{U,R_m})^T$ for U using the observation R_m and satellites $(S^{b_n}_{2n-1,2n}, S^{b_n}_{2n,2n-1})$. The statistical and final position and velocity of U using all R_m's are $\mathbb{E}[\dot{r}_U] = \frac{1}{M}\sum_{m=1}^{M} \dot{r}_U$ and $\mathbb{E}[\dot{v}_U] = \frac{1}{M}\sum_{m=1}^{M} \dot{v}_U$ are used as $\hat{r}_U$ and $\hat{v}_U$, respectively. After obtain all the solutions for U using all R_m, where $m \in \{1, ..., M\}$ for each $(S^{b_n}_{2n-1,2n}, S^{b_n}_{2n,2n-1})$, where $n \in \{1, ..., N\}$ the next step is to calculate the from **Eq. 6** and **Eq. 7** the single difference (SD) to find the only unknown TE: $\delta t_{U,R_m} = \delta t_U - \delta t_{R_m}$ from:

$$
\begin{aligned}
\phi^{S^{b_n}_{2n-1,2n}}_{U,R_m,L_i} &= \frac{c}{\lambda_{L_i}}(t_U - t_{R_m}) + \frac{c}{\lambda_{L_i}}(\delta t_U - \delta t_{R_m}) \\
&\quad + (\phi^{(0)}_{U_{L_i}} - \phi^{(0)}_{R_{m,L_i}} + \dot{N}^{S^{b_n}_{2n-1,2n}}_{U,R_m,L_i})
\end{aligned} \tag{14}
$$

Lastly, after obtaining all the solutions $\delta t_{U,R_m}$ for each binary satellite formation $(S^{b_n}_{2n-1,2n}, S^{b_n}_{2n,2n-1}), n \in \{, ..., N\}$, the final solution is the following:

$$
\begin{aligned}
\bar{\delta t}_{U,R_m} &= \mathbb{E}[\delta t_{U,R_m}] \\
&= \frac{1}{N}\sum_{n=1}^{N}(\delta t_U - \delta t_{R_m})^{(S^{b_n}_{2n-1,2n}, S^{b_n}_{2n,2n-1})}
\end{aligned} \tag{15}
$$

The summary of the proposed algorithm is at **Alg. 1**

Algorithm 1 Time Error $\delta t_{U,R_m}$ evaluation between UE GNSS receiver $U$and the 5G BBU GNSS receiver R_m local clocks

Initialization: {
a) Reading GNSS signal raw broadcasting measurements for phase-range and Pseudo ranges for the U and R_m:($\boldsymbol{\Phi_{L_1}}$,...,$\boldsymbol{\Phi_{L_i}}$,...,$\boldsymbol{\Phi_{L_I}}$,$\boldsymbol{P_{L_1}}$,...,$\boldsymbol{P_{L_i}}$,...,$\boldsymbol{P_{L_I}}$)
b) Allocate the best two binary Satellite systems in respect to U sky azimuth view
c) Allocate M BSs that satisfy the condition : The U is located in the center of the BSs locations, and the R_ms are equally far from each other.
}
for epoch k **do**
  for each $R_m, m \in \{1, ..., M\}$ **do**
    for each $(S^{b_n}_{2n-1,2n}, S^{b_n}_{2n,2n-1}), n \in \{1, ..., N\}$ **do**
      calculate the initial geometrical locations of ρ_U, ρ_{R_m} using classical Single Point Positioning and the accurate R_m location, respectively [10].
      Predict by EKF the initial float ambiguity resolution $\hat{N}_{U,R_m}$.
      Send the Measurements and Observations to the RTK algorithm
      Use the Modified Lambda algorithm to solve the ILS problem and find the ambiguity resolution $\dot{N}_{U,R_m}$.
      Use the calculated $\dot{N}_{U,R_m}$ to find the $\delta t_{U,R_m}$ in **Eq. 14**.
    end for
    Find $\bar{\delta t}_{U,R_m} = \mathbb{E}[\delta t_{U,R_m}]$ using **Eq. 15**.
  end for
  Find $\mathbb{E}[\dot{r}_U]$ and $\mathbb{E}[\dot{v}_U]$
end for
Output: $\bar{\delta t}_{U,R_m}$.

IV. Simulation Setup and Experiment Parameters

In this paper, the MATLAB simulation considers two formations of binary satellite systems $(S^{b_n}_{2n-1,2n}, S^{b_n}_{2n,2n-1})$, where $n \in \{1, 2\}$ and three BS references to calculate and evaluate the position accuracy in ECEF for one U and the TE between U and each R_m, where $m \in \{1, 2, 3\}$. The synthesized ground truth data consist of the three stationary BSs locations in geodetic latitude, longitude, altitude (LLA) coordinates and a ground truth trajectory for one UE in LLA and constant velocity vector. **Table. I** summaries the most important parameters used in the simulation.

TABLE I
Parameters used for simulations

Parameter	Value
GNSS system	GPS
Carrier frequency	$f_c = 1575.42$
Short base distance	100 meters
Carrier-Phase Bias noise	$\sigma_{\varepsilon_\phi} = 10^{-3}$ Cycle
Ionospheric Delay noise	$\sigma_I = 10^{-3}$m/10 Km
Tropospheric Delay noise	$\sigma_T = 10^{-4}$ m
No. of experiments (Monte-Carlo Sim.)	10000 samples

V. Simulation Results and Discussion

By using Monte-Carlo simulation to repeat 10'000 experiments for ECEF 'U' positioning error in comparison to the ground truth and TE in $\bar{t}_{U,R_m}$: the results in **Fig. 2** shows that the RTK algorithm in blue lines outperforms the classical single point positioning using the GPS data only in black lines. However, the proposed algorithm with binary satellite formation systems and multi references improves the U positioning accuracy in green lines. The accuracy of the proposed algorithm at **Fig. 3** shows the approximate improvement of 1.5 centimeters in comparison to the conventional RTK algorithm. The explanation of such an improvement that the symmetrical geometry of binary satellite formation with respect to U reduces $I^{S^{b_n}_{2n-1,2n}}_{R_m,L_i}$, $T^{S^{b_n}_{2n-1,2n}}_{R_m}$, and $\lambda_{L_i} B^{S^{b_n}_{2n-1,2n}}_{R_{m,L_i}}$ in **Eq. 9**. In addition, the three R_m used to correct the location U are improving the SD ambiguity $\dot{N}_{U,R_m}$ and reducing the σ^s_{Φ,L_i} and pseudo-range σ^s_{P,L_i} noises, also improving of theEKF the U velocity system east, north and up noises (σ_{ve},σ_{vn},σ_{vu}) between the epochs t_k and t_{k+1}. Which produces more accurate positioning capabilities for U than the conventional RTK. Finally, in **Fig. 4** the improvement in measuring the clock time difference between the 'U' and the R_m in comparison with both the classical GPS and RTK algorithms shows a better performance. Furthermore, the range of TE difference is within ± 10 ps. This timing accuracy results from obtaining a higher baseline accuracy between the U and the R_m using the correction observations from all R_m.

VI. Conclusion

This paper investigates improving the positioning and TE for the UE U as a rover by proposing spatially correlated satellites as a binary formation system. Furthermore, helping

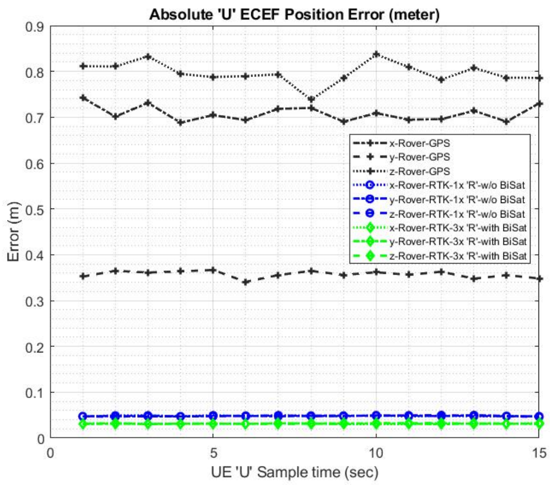

Fig. 2. Positioning Error in U ECEF coordinates

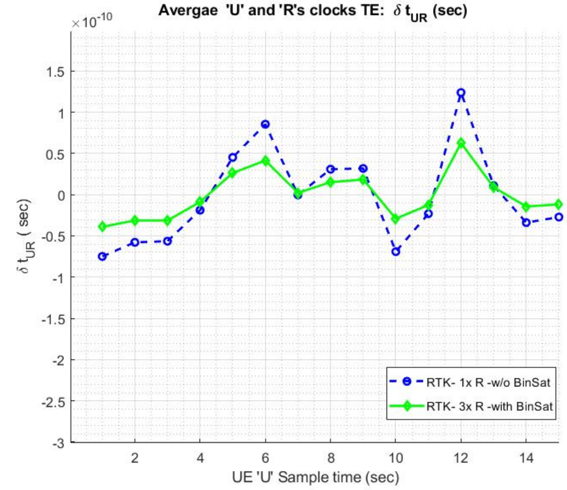

Fig. 4. System Model for Multi-Reference RTK Algorithm

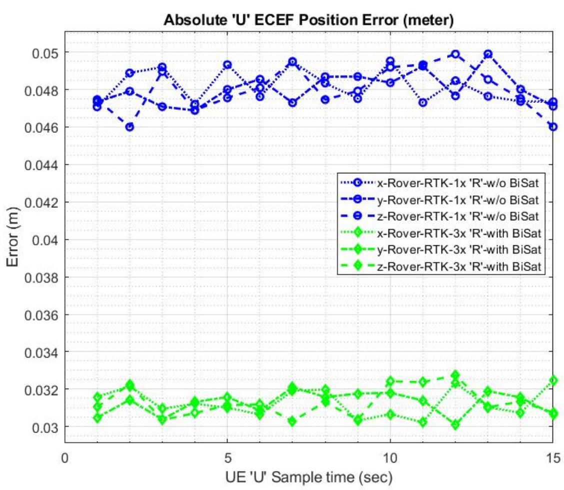

Fig. 3. RTK vs RTK with Multi R_m and Binary Sat. Positioning Error for U ECEF coordinates

to obtain U correction observations using more than one BS increases positioning accuracy, improves the TE between the local clocks of the UE and the BS, and maintains within the sub-nanosecond range.

REFERENCES

[1] L. Dai, D. Eslinger, and T. Sharpe, "Innovative algorithms to improve long range rtk reliability and availability," in *Proceedings of the 2007 National Technical Meeting of the Institute of Navigation*, 2007, pp. 860–872.

[2] F. Alriksson, L. Boström, J. Sachs, Y. Wang, and A. Zaidi, "Critical iot connectivity: Ideal for time-critical communications," *Ericsson technology review*, 2020.

[3] S. Ruffini, M. Johansson, B. Pohlman, and M. Sandgren, "5g synchronization requirements and solutions," *Ericsson technology review*, 2021.

[4] C. Rizos, "Precise gps positioning: Prospects and challenges," in *Proceedings of the fifth international symposium on satellite navigation technology & applications, Canberra*. Citeseer, 2001.

[5] J. Fischer and P. Myers, "Sub-nanosecond timing sync using rtk receivers," in *Proceedings of the ION 2013 Pacific PNT Meeting*, 2013, pp. 584–587.

[6] X. Mi, B. Zhang, and Y. Yuan, "Stochastic modeling of between-receiver single-differenced ionospheric delays and its application to medium baseline rtk positioning," *Measurement Science and Technology*, vol. 30, no. 9, p. 095008, 2019.

[7] L. L. Dai, D. J. Eslinger, R. T. Sharpe, and R. R. Hatch, "Partial search carrier-phase integer ambiguity resolution," Jun. 14 2011, uS Patent 7,961,143.

[8] K. Alemdar, D. Varshney, S. Mohanti, U. Muncuk, and K. Chowdhury, "Rfclock: timing, phase and frequency synchronization for distributed wireless networks," in *Proceedings of the 27th Annual International Conference on Mobile Computing and Networking*, 2021, pp. 15–27.

[9] S. Fan, W. Ni, H. Tian, Z. Huang, and R. Zeng, "Carrier phase-based synchronization and high-accuracy positioning in 5g new radio cellular networks," *IEEE Transactions on Communications*, vol. 70, no. 1, pp. 564–577, 2021.

[10] T. Takasu, "Rtklib ver. 2.4. 2 manual, rtklib: An open source program package for gnss positioning, 2013," *Paper available at website: http://www. rtklib. com/prog/manual_2*, vol. 4.

[11] A. Gelb *et al.*, *Applied optimal estimation*. MIT press, 1974.

[12] X.-W. Chang, X. Yang, and T. Zhou, "Mlambda: A modified lambda method for integer least-squares estimation," *Journal of Geodesy*, vol. 79, no. 9, pp. 552–565, 2005.